

17. Wong, L. S., Johnson, M. S., Zhulin, I. B. & Taylor, B. L. Role of methylation in aerotaxis in *Bacillus subtilis*. *J. Bacteriol.* **177**, 3985–3991 (1995).
18. Taylor, B. L. & Zhulin, I. B. PAS domains: internal sensors of oxygen, redox potential, and light. *Microbiol. Mol. Biol. Rev.* **63**, 479–506 (1999).
19. Zhulin, I. B. & Taylor, B. L. Correlation of PAS domains with electron transport-associated proteins in completely sequenced microbial genomes. *Mol. Microbiol.* **29**, 1522–1523 (1998).
20. Gilles-Gonzalez, M. A., Ditta, G. S. & Helinski, D. R. A haemoprotein with kinase activity encoded by the oxygen sensor of *Rhizobium meliloti*. *Nature* **350**, 170–172 (1991).
21. Monson, E. K., Weinstein, M., Ditta, G. S. & Helinski, D. R. The FixL protein of *Rhizobium meliloti* can be separated into a heme-binding oxygen-sensing domain and a functional C-terminal kinase domain. *Proc. Natl Acad. Sci. USA* **89**, 4280–4284 (1992).
22. Zhulin, I. B., Taylor, B. L. & Dixon, R. PAS domain S-boxes in *Archaea*, *Bacteria* and sensors for oxygen and redox. *Trends Biochem. Sci.* **22**, 331–333 (1997).
23. Gong, W. *et al.* Structure of a biological oxygen sensor: a new mechanism for heme-driven signal transduction. *Proc. Natl Acad. Sci. USA* **95**, 15177–15182 (1998).
24. Rebbapragada, A. *et al.* The Aer protein and the serine chemoreceptor Tsr independently sense intracellular energy levels and transduce oxygen, redox, and energy signals for *Escherichia coli* behavior. *Proc. Natl Acad. Sci. USA* **94**, 10541–10546 (1997).
25. Bibikov, S. I., Biran, R., Rudd, K. E. & Parkinson, J. S. A signal transducer for aerotaxis in *Escherichia coli*. *J. Bacteriol.* **179**, 4075–4079 (1997).
26. Vagner, V., Dervyn, E. & Ehrlich, S. D. A vector for systematic gene inactivation in *Bacillus subtilis*. *Microbiology* **144**, 3097–3104 (1998).
27. Leonhardt, H. & Alonso, J. C. Construction of a shuttle vector for inducible gene expression in *Escherichia coli* and *Bacillus subtilis*. *J. Gen. Microbiol.* **134**, 605–609 (1988).
28. Alam, M. & Hazelbauer, G. L. Structural features of methyl-accepting taxis proteins conserved between archaeobacteria and eubacteria revealed by antigenic cross-reaction. *J. Bacteriol.* **173**, 5837–5842 (1991).

Acknowledgements

We thank H. G. deCouet, S. Donachie, G. L. Hazelbauer, M. Manson and O. R. Zaborsky for helpful comments on the manuscript, A. Brooun for the *hemAT-Hs* deletion strains, H. Chen and J. Yang for participation in the initial stage of protein purification, T. Freitas for preparing Fig. 1, and J. Spudich for the shuttle vector pKJ427. This investigation was supported by National Science Foundation CAREER grant to M.A. *HemAT-Hs* (HtB) has been given GenBank accession number U75436, and *HemAT-Bs* (YhfV) GenBank accession number Y14084.

Correspondence and requests for materials should be addressed to M.A. (e-mail alam@hawaii.edu).

Motor disorder in Huntington's disease begins as a dysfunction in error feedback control

Maurice A. Smith*, Jason Brandt† & Reza Shadmehr*

* Department of Biomedical Engineering and † Department of Psychiatry and Behavioral Sciences, Johns Hopkins University, Baltimore, Maryland 21205-2195, USA

A steady progression of motor dysfunction takes place in Huntington's disease¹ (HD). The origin of this disturbance with relation to the motor control process is not understood. Here we studied reaching movements in asymptomatic HD gene-carriers (AGCs) and subjects with manifest HD. We found that movement jerkiness, which characterizes the smoothness and efficiency of motion, was a sensitive indicator of presymptomatic HD progression. A large fraction of AGCs displayed elevated jerk even when more than seven years remained until predicted disease onset. Movement termination was disturbed much more than initiation and was highly variable from trial to trial. Analysis of this variability revealed that the sensitivity of end-movement jerk to subtle, self-generated early-movement errors was greater in HD subjects than in controls. Additionally, we found that HD corrective responses to externally-generated force pulses were greatly disturbed, indicating that HD subjects display aberrant responses to both external and self-generated errors. Because feedback corrections are driven by error and are delayed such that they

predominantly affect movement termination, these findings suggest that a dysfunction in error correction characterizes the motor control deficit in early HD. This dysfunction may be observed years before clinical disease onset and grows worse as the disease progresses.

Huntington's disease is an autosomal dominant inherited neurological disorder caused by a glutamate repeat expansion in the IT15 gene². Disease symptoms appear in the fourth or fifth decade of life¹,

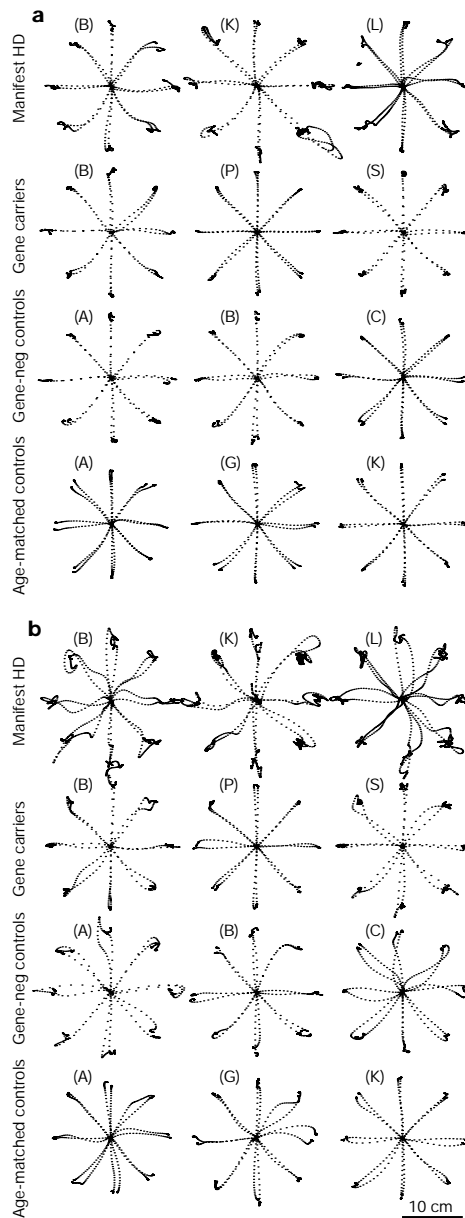


Figure 1 Hand paths from selected subjects after 200 practice trials (movements 201–300). **a**, The two most regular movements in each direction. **b**, The two least regular movements each direction. Movement regularity was determined by the correlation coefficient⁶ of the velocity profile with the velocity profile of that subject's typical movement. The typical movement was defined as the movement in each direction with the highest average correlation to other movements. Hand paths are plotted from the centre out relative to their starting positions. Points are spaced 30 ms apart in time. The distance between consecutive points is proportional to the movement speed during that interval. Top row, subjects with manifest HD. Second row, asymptomatic gene-carriers. Third row, controls who have a parent with HD but who are mutation negative. Bottom row, controls age-matched to the asymptomatic gene-carriers. The letter that labels each subject identifies him or her within each group in Fig. 2.

and then progress steadily during the succeeding 10–20 years. Significant, progressive atrophy of the basal ganglia is evident in HD (ref. 3), and may even be detectable before clinical onset⁴. Its identifying motor sign is chorea: the occurrence of rapid, irregular, and arrhythmic complex involuntary movements. Along with chorea, substantial impairment of voluntary movement also occurs¹, and it may be of greater functional importance in the lives of patients⁵. Two control processes take part in the execution of arm movements. Feedforward control is the generation of motor commands based a priori on the desired action and an internal model of the system's response^{6,7}, whereas feedback control entails the 'mid-flight' correction of these commands based on errors detected during their execution⁸. To study these processes in HD, we used a high-performance manipulandum⁹ to record visually guided reaching arm movements in patients with HD and pre-symptomatic individuals with the HD mutation up to 18 years from predicted disease onset.

Figure 1 displays hand paths of the two most regular and two least regular movements in each direction, for several subjects after 200 practice movements. The range of movement quality is generally much larger in HD patients than in controls. Some movements made by symptomatic HD subjects appear normal whereas others are markedly irregular. Specifically, many HD movements have large changes in direction, smooth or abrupt, when approaching the target, whereas almost all movements fail to stop efficiently and smoothly. One way to characterize these irregularities is to quantify the smoothness of each movement. Smoothness can be defined as the lack of abrupt change; thus a trajectory that minimizes abrupt changes in a variable will maximize its smoothness. Human reaching movements are of near-maximal acceleration smoothness, quantified by minimal cumulative squared acceleration change¹⁰, also referred to as minimum total squared jerk.

Figure 2a shows that all HD patients and several AGCs made movements with above-normal jerk. All HD subjects reduced their movement jerk with practice, although not nearly to control levels. The smoothness of movements increased over time even in subjects who were markedly more jerky than normal. To compare the initiation and completion of movement, we split each movement at the peak in the speed profile. This is roughly the point at which movement towards the target switches from acceleration to deceleration. Comparison of the total squared jerk before and after the peak in the speed profile (Fig. 2b) reveals that although fewer than half of the HD patients have high jerk during both parts of the movement, all have above-normal post-peak jerk. Only 2 of 16 AGCs show above-normal pre-peak jerk, but most have high post-peak jerk. To assess disease progression in AGCs, we used an estimate of disease onset age based on each subject's parental onset age and glutamate repeat length⁴. The amount of post-peak jerk correlated significantly ($r = -0.62$) with estimated time to disease onset for AGCs whereas the pre-peak jerk did not ($r = 0.02$). Post-peak jerk was above normal in 4 of 5 close-to-onset (<7 years) subjects and in 3 of 9 far-from-onset (>7 years). As groups, both HD patients and AGCs had significantly higher than normal post-peak jerk ($P < 10^{-6}$, $P < 0.00012$; see Fig. 2e). Moreover, AGCs who were close to predicted disease onset had significantly higher jerk in the third set than far-from-onset subjects ($P < 0.0062$) who in turn had significantly higher jerk than controls ($P < 0.013$).

Figure 2c shows that initial aiming is not greatly disturbed in HD. Average directional aiming bias (see Methods section) is normal in 9 of 11 HD patients. Aiming variability is in the control range for a majority (6 of 11) of patients, although, as a group, subjects with manifest HD display increased aiming variability. All AGCs have normal aiming biases of 3–7° and none has above-normal aiming variability.

These results suggest that HD movements often begin normally, but become jerky and irregular at some point during their course. Comparison of the average time course of raw squared jerk profiles

between groups for movements in different speed ranges (Fig. 3) reveals a strikingly consistent pattern. At each speed range, the HD jerk profile closely matches the control profile during the beginning of movement, but begins to separate from it 200–300 ms after onset. Note that the end-movement squared jerk is 10–30 times greater in HDs than controls.

Why do HD movements begin to become irregular 200–300 ms into their course and not before? Corrective actions based on visual^{11,12} and proprioceptive¹³ information acquired during reaching movements begin to take place at about the time at which HD movements become irregular, so one possibility is that the system that generates these corrective actions is disturbed. Alternatively, there may be a disturbance in decelerating movement or another end-movement process independent of error correction.

To distinguish between these possibilities, we characterized the performance of the error feedback control system in HD. If the system that generates corrective actions during movement (the feedback controller) is affected in HD, then a strong relationship should exist between magnitude of error early in the movement and size of disturbance later. Error, the difference between desired system state and actual state, is the primary input to a feedback controller. If the error during a movement is small, then large

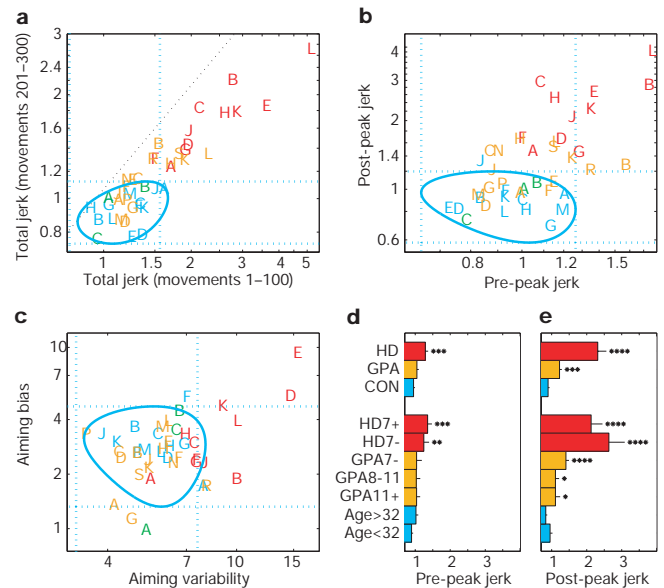


Figure 2 Quantification of movement properties. Red, subjects with manifest HD. Orange, asymptomatic gene-carriers. Blue, age-matched controls. Green, gene-negative individuals having a parent with HD. **a–c** are plotted on a logarithmic scale for clarity. The blue dotted lines show the 95% confidence intervals for the control distribution (mean ± 1.96 standard deviations). The black diagonal line in **a** represents the axis of equality ($y = x$). **a**, The mean of the normalized total squared jerk for all subjects in the first 100 movements and in movements 201–300. All symptomatic subjects and a subset of asymptomatic gene-carriers have higher than normal jerk. **b**, The mean of normalized jerk (in movements 201–300) before and after the peak in the movement speed. The pre-peak segment, which reflects movement initiation, appears much less disturbed in HD than the post-peak segment, which reflects movement completion. **c**, Aiming bias and aiming variability. We refer to aiming as the direction of travel with respect to the initial target direction, during the pre-peak movement segment. Like pre-peak jerk, aiming reflects the quality of movement. **d,e**, Group-wise comparisons of normalized pre-peak and post-peak jerk, respectively. Asterisks indicate significantly worse performance than control subjects. * $P < 0.05$. ** $P < 0.01$. *** $P < 0.001$. **** $P < 0.0001$. HD7+, subjects with manifest HD for more than 7 years. HD7–, subjects with manifest HD for less than 7 years. GPA7–, gene-carriers less than 7 years from predicted onset. GPA7–11, gene-carriers 7 to 11 years from predicted onset. GPA11+, gene-carriers more than 11 years from predicted onset. Age > 32, controls more than 32 years old. Age < 32, controls less than 32 years old.

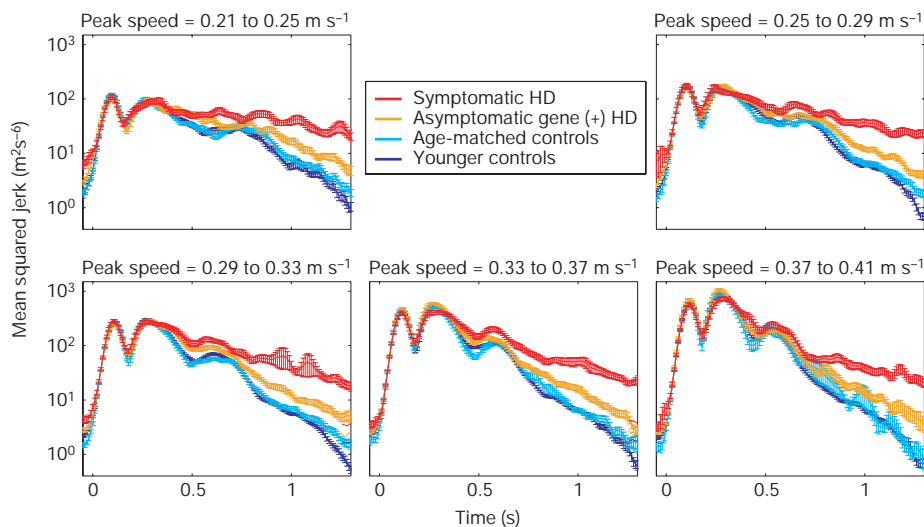


Figure 3 Squared jerk profiles for different movement speeds. Average raw squared jerk \pm standard error is plotted on a logarithmic scale as function of time since movement onset for movements in each speed range, in different subject groups. For reference, the

second peak in the squared jerk profile approximately corresponds to the peak in the speed profile. Note that at all speed ranges the separate groups have quite similar jerk profiles until 300 ms, but HD subjects have very different profiles after this point.

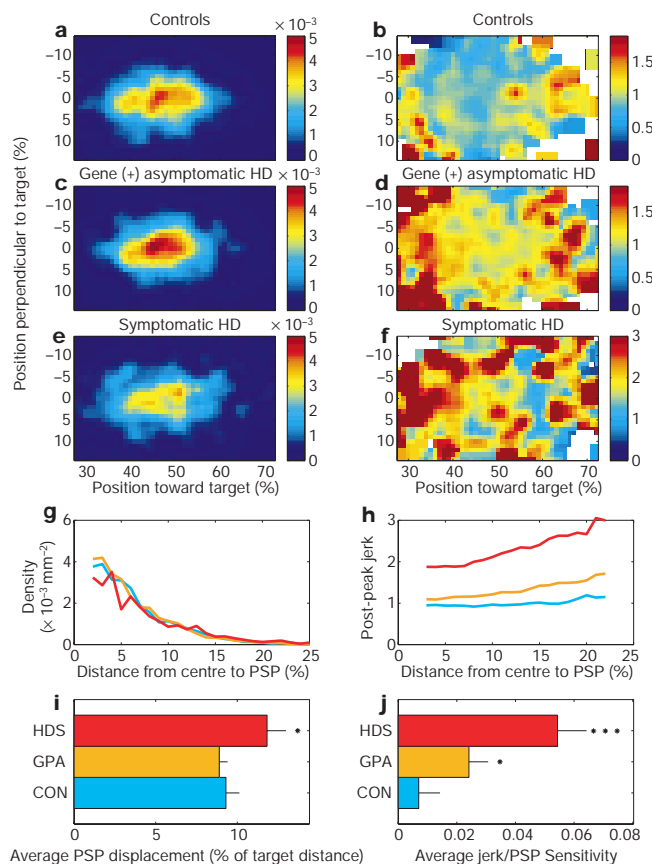


Figure 4 Errors that occur early in the movement, before the hand reaches its peak speed, predict jerk that occurs later. **a,c,e**, The two-dimensional probability densities of peak speed positions (PSPs) for each group during movements 301–400. This is the likelihood of the peak speed occurring at each position. The x-axes are in the target direction and the y-axes are in the direction perpendicular to the target. PSPs are clustered near the movement midway point. **g**, Summary of **a,c,e**: the average probability density at a given displacement between the PSP and movement midway point (50%, 0%). Large values for the distance from midway point to peak-speed position indicate large early-movement errors, which are uncommon. The similarity of these distributions indicates that there are not large differences in the pattern of error recorded from the three subject groups early in

the movement. **b,d,f**, End-movement jerk as a function of peak-speed position. When large early movement errors occur, as indicated by large PSP displacements (near the image boundaries), the post-peak jerk is increased for all groups, but the increase is greater for asymptomatic and symptomatic HD subjects than controls. White colour on images indicates no data. **h**, Summary of **b,d,f**: the average end-movement jerk at a given displacement between the PSP and movement midway point. **i**, Average PSP displacement for each group. **j**, Sensitivity of end-movement jerk to PSP, measured as the slope of the relationship between them. Asterisks indicate significantly worse performance than control subjects. * $P < 0.05$. ** $P < 0.01$. *** $P < 0.001$.

corrective actions are not necessary and dysfunction in feedback control might have only minimal effects. However, if errors are large, substantial corrective actions are required, and dysfunctional feedback control may cause significant problems with movement.

Although we can measure actual movements quite accurately, we have no reliable way of estimating the desired motion state within a single movement. This makes direct estimation of error infeasible. If errors are symmetrically distributed, then the average movement profile should approximate the average motion plan (that is, the average intended movement of the subject). However, subjects may plan to move slightly faster on one trial, then slower on the next, and these variations in the plan may be as large as the typical errors between plan and action. Although the motor plan might change across trials, a few of its properties are invariant. Velocity profiles of reaching movements are symmetric and unimodal: the peak in the velocity profile occurs very close to the movement's midway point, regardless of amplitude, direction or speed¹⁴. Therefore, the distance between the midway point and the position where the peak speed occurs can be used as an indicator of error early in the movement.

The relationship between error early in movement and jerk late in movement is shown in Fig. 4. The probability distributions of peak-speed positions (PSPs) do not differ markedly between groups (Fig. 4 a,c,e,g and i). This implies that amount of error early in the movement is comparable between groups. However, the reaction to this error is very different between groups. Figure 4 b,d,f,h and j shows that the jerk that occurs after the hand reaches the PSP varies considerably with PSP in all subject groups. When the PSP is far from the midway point, indicating large error early in the movement, post-peak jerk is high. However, the sensitivity of post-peak jerk to PSP is much greater in HD patients and AGCs than controls. Figure 4h shows that the difference in mean post-peak jerk between

controls and AGCs is much greater at large PSP displacements than at small displacements. Subjects with manifest HD ($P = 0.006$) and AGCs ($P = 0.04$) display significantly higher sensitivity in their response of end-movement jerk to early-movement error than do controls, as measured by slope in this relationship. The sensitivity of post-peak jerk to PSP displacement indicates the degree to which end-movement smoothness depends on early-movement error. The increase in this sensitivity in HD subjects with and without clinically manifest symptoms suggests that an error-dependent control process is disturbed early in the disease course and further deteriorates with disease progression.

Previous reports have shown that cortical sensorimotor pathways are affected in patients with manifest HD. Whereas short-loop reflexes that are mediated by spinal mechanisms are normal, long-loop reflexes, which involve the transfer of proprioceptive information through cortical pathways, are reduced or absent in HD^{15,16}. Cortical responses to peripheral nerve stimulation, as measured by somatosensory evoked potentials (SEPs), are also reduced in HD^{15,17,18}, suggesting that diminished cortical sensory input is responsible for the long-loop reflex reduction¹⁶. In addition, a strong correlation exists between SEP deterioration and striatal glucose metabolism early in the course of HD¹⁷, hinting at a possible involvement of the striatum in the pathology of the SEPs and long-loop reflexes. As cortical sensorimotor pathways have a large role in mediating error correction during voluntary movement, disruption of these pathways could lead to dysfunctional feedback control during movement.

Our analysis of the response to internal, self-generated errors suggested that error correction in general might be disturbed in HD. To test this hypothesis we externally imposed errors upon movements of these subjects via an occasional brief (70 ms) force pulse shortly after movement initiation. These pulses were given

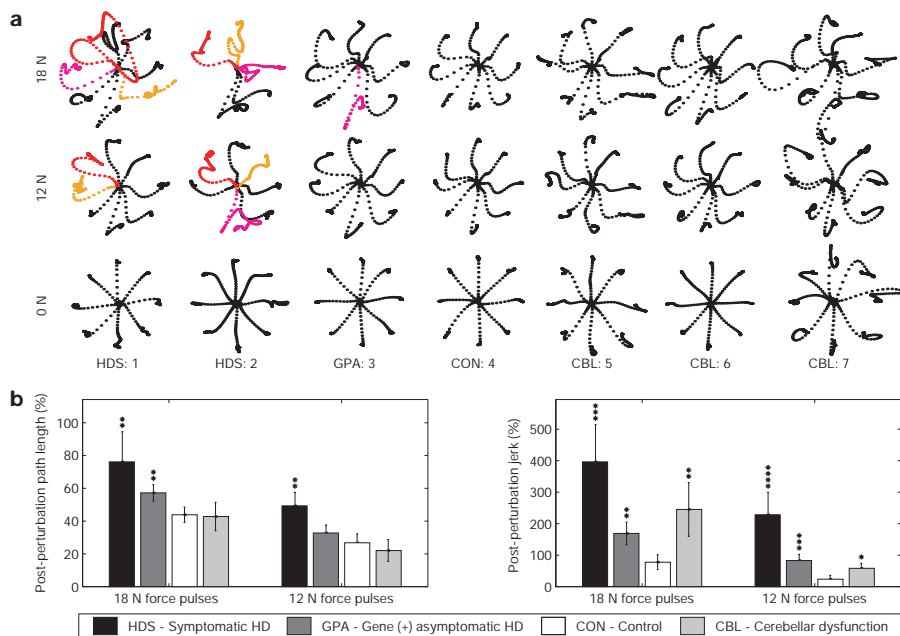


Figure 5 Force-pulse perturbations disturb the movements of HD subjects more than controls or cerebellar subjects. **a**, Sample movement trajectories during the perturbation task. Top two rows, movements during which an 18 or 12 N force pulse was applied in the 7:30 direction. Bottom row, typical unperturbed movements interspersed within the perturbed movements. Some of the movements made by HD subjects become greatly disturbed after a perturbation is applied. A few of the most greatly disturbed trajectories are highlighted. Note the trajectory towards 10:30 for HD subject 1. Here the movement begins in the correct direction but is perturbed to the left. The 'correction' then brings the

movement quickly back all the way past the original starting location, turns around and heads roughly towards the target, then makes a final turn, moves towards the target and stops. **b**, Change in movement properties in response to force-pulse perturbations (% change with respect to unperturbed movements). Right panel, normalized post-perturbation path length. Left panel, normalized post-perturbation jerk. Asterisks indicate significant increases above control disturbance. * $P < 0.05$. ** $P < 0.025$. *** $P < 0.01$. **** $P < 0.001$.

randomly on a minority of trials, and could be in eight different directions (indicated by the times corresponding to clockface directions) and of three different magnitudes (6, 12 and 18 N peak force). In addition to subjects with HD, we studied the performance of individuals with cerebellar deficits on this task. Hand paths of two symptomatic HD, one AGC, one control and three cerebellar subjects for movements perturbed with force pulses of 12 and 18 N are shown in Fig. 5a. These perturbations are substantial: trajectories can be altered by up to 5 cm (movement distance is 10 cm). Control subjects correct the perturbations smoothly and efficiently, but extremely large successive overshoots are seen during certain HD movements. Not all HD movement corrections appear irregular, but some are so markedly disturbed that they bear little qualitative similarity to any movements that we recorded from controls.

Several movements made by cerebellar subjects appear to have irregular and inefficient corrections, but close inspection of many of these trajectories reveals a striking similarity between the pattern of overshoots in these movements and the overshoots present in unperturbed movements in the same direction. This suggests that the irregularity that exists in these perturbed movements has a stronger relationship to the direction of movement than to the presence of perturbation. We note that such movements toward 3:00, 4:30 and 7:30 for subjects 5 and 7.

HD subjects appear to have dysfunctional reactions to movement errors caused by external perturbations. During the post-perturbation movement segment (the corrective period), jerk and path length relatively increase over unperturbed movements significantly more for HD subjects than for controls (see Fig. 5b) for both 12- and 18-N perturbations. The error-correction performance of AGCs generally falls between that of controls and subjects with manifest HD. Cerebellar subjects, like symptomatic HD patients, had worse unperturbed movement performance than controls, but the decrement in their performance when perturbations were given was generally more like that of controls than HD subjects. This suggests that subjects with HD generally have greater deficits in error feedback control than do cerebellar patients.

Previously, assessments of motor, cognitive or psychiatric function in HD have revealed only subtle deficits in presymptomatic subject groups^{19–21} if any^{22,23}. When changes have been detected, they were not sufficiently specific to permit discrimination between mutation-positive and mutation-negative individuals, or even reliable identification of people with early-stage manifest HD. In contrast, low glucose metabolism in the basal ganglia has been reported in about two-thirds of asymptomatic at-risk individuals tested^{17,24,25} and basal ganglia volumes may be reduced years before clinical onset⁴, suggesting that brain pathology precedes manifestation of the behavioural dysfunction previously studied. However, end-movement jerk appears to be a sensitive indicator of HD progression, suggesting the existence of a direct behavioural correlate to the early brain pathology of HD.

Our results, which suggest relatively unaffected feedforward control but dysfunctional feedback control in HD, may help to explain the pattern of motor learning deficits reported: learning rotary pursuit, which involves long continuous movements under closed-loop feedback control, is more impaired than mirror tracing with short discrete movements that are more open-loop in nature²⁶. Real-time error feedback control presents a formidable challenge to the CNS because of the large sensorimotor delays that occur²⁷. One way to improve the performance of such a time-delayed system is to include a component that can effectively predict away the delay and allow efficient error correction. This sort of predictor has been referred to as a forward model of system dynamics^{8,28}. Neurons in the basal ganglia have been shown to predict reward by firing vigorously in advance of reward upon completion of the requirements for reward attainment²⁹, hinting that predictive capacity may be a general feature of some basal ganglia structures. The main

output of the basal ganglia modulates the action of the thalamus, which relays sensory information to the cortex. This information stream is likely to participate in error feedback control. □

Methods

Subjects

Eleven patients positive for the IT-15 mutation and symptomatic with Huntington's disease, sixteen mutation-positive presymptomatic subjects, three mutation-negative subjects who had a parent with HD and twelve other age-matched controls participated in the first experiment. Five symptomatic and nine presymptomatic HD subjects, eight age-matched controls and six subjects with cerebellar lesions participated in the second experiment. All subjects used their dominant hand, and all but one presymptomatic subject in the first experiment were right-handed. The direct gene test for IT-15 mutation was conducted at the Johns Hopkins Huntington's Disease Project. The number of CAG (glutamate) trinucleotide repeats was determined, and subjects with >37 repeats were called mutation-positive. Subjects with <34 were called mutation-negative. All cerebellar subjects that we studied had been diagnosed clinically with cerebellar dysfunction, and all had lesions localized to the cerebellum on MRI. Four patients had generalized cerebellar atrophy, and two had suffered strokes of the right posterior inferior cerebellar artery (PICA). One of these patients also had a left PICA and a right superior cerebellar artery stroke.

Task

Subjects made quick reaching movements to targets spaced 10 cm away while grasping a lightweight two-joint manipulandum. The 1-cm square targets and a small cursor indicating the subject's hand position were displayed on a computer monitor in front of the subject⁶. We define the end of the movement as the beginning of the first time interval after movement onset when hand velocity always remained below a threshold of 0.03 m s^{-1} for 200 ms. During the first experiment, the training took place in two sessions and within sessions it was subdivided into 100-movement sets. In the first session, subjects completed three sets of training. After a break of 3–4 hours, they began the second session, which consisted of a single set. The robot arm remained passive for all movements in both sets. During the second experiment the robot produced a 70-ms bell-shaped force pulse on a minority of randomly pre-selected trials (with a probability of one in four). The force pulse could be in any one of eight directions and of magnitude 6, 12 or 18 N. One force pulse in each direction and of each magnitude was given for each direction of movement. During both experiments we used a sling suspended from the ceiling to support the subject's upper arm in the horizontal plane. This helped to regularize the subjects' arm position and minimize the effort required to support the arm against gravity.

Analysis

We characterized aiming direction by defining angular aiming error as the difference between target direction and the direction of travel up to the peak speed point. Aiming error for a given movement can be positive or negative. Aiming bias for each subject was defined as the average of the magnitude of the average aiming error in each direction. Similarly, aiming variability for each subject was defined as the average of the standard deviation of aiming error in each direction.

Jerk is defined as the rate of change of acceleration with respect to time. To minimize the effect of discretization noise on the differentiation of the velocity signal, jerk was estimated by applying a Savitsky–Golay filter. The minimum total squared jerk (TSJ) required for a point-to-point movement is proportional to the fifth power of the movement speed and inversely proportional to the third power of movement excursion. Because of the strength of the relationship between these variables and TSJ, it is critical to normalize movement speed and excursion appropriately when comparing the amount of jerk between two movements. To account for the effect of speed and excursion on a movement's typical jerk, we normalized the TSJ measured for each movement by the average TSJ for movements made after practice by a large separate group of controls ($n=35$), at the appropriate speed and excursion. Similarly, we normalized the TSJ in the pre-peak and post-peak movement segments by the average values of these quantities for control movements of the same peak speed and excursion, and we refer to these quantities as pre-peak jerk and post-peak jerk.

As the trajectories of perturbed movements were often quite irregular, and the peak speed was often strongly influenced by the presence and direction of the perturbing force pulse, normalization of jerk by peak speed was no longer appropriate for these movements. Instead, we normalized the jerk measured after a perturbation offset for a given movement by dividing by the minimum possible jerk required to make the movement state transition characteristic of that movement segment. We refer to this quantity as post-perturbation jerk. Similarly, we define post-perturbation path length as the path length between the point of perturbation offset and the end point of movement divided by the straight-line distance between these two points. We compare the values of these quantities for movements during which perturbations were given to unperturbed movements. For unperturbed movements, we define the time point of 'perturbation offset' as that time when perturbation offset would have occurred had a perturbation been given.

Analytical methods

The position and velocity of the joints of the robot arm were recorded at 100 Hz from absolute and relative joint position encoders with resolution of 5.5×10^{-3} degrees and 8.0×10^{-4} degrees, respectively. This produced estimates of hand position and

velocity in cartesian coordinates with accuracy greater than 0.1 mm and 1.3 mm s⁻¹, respectively.

Jerk was estimated by applying a fourth-order Savitsky–Golay filter on a 250-ms window of velocity data. This filter is equivalent to taking the second derivative at the window's centre of the continuous least-squares best-fit fourth-order polynomial. This fourth-order polynomial fit is a low-pass filter with a cutoff frequency of 6.83 Hz. Power spectra of mean subtracted velocity profiles of very fast 10-cm reaching movements show that 99.9% of the power is below 6 Hz.

We assessed motion state transition efficiency using cumulative squared jerk to characterize the efficiency of recovery after perturbation offset. To accomplish this, we compared the amount of jerk that occurred between two different motion states within the same movement, with the jerk that would occur for a maximally smooth transition between those two states in the elapsed time. The minimum jerk trajectory between two motion states (state = [position, velocity, acceleration]) is given by a fifth-order polynomial in time:

$$x(t) = C_5(t/t_f)^5 + C_4(t/t_f)^4 + C_3(t/t_f)^3 + C_2(t/t_f)^2 + C_1(t/t_f) + C_0$$

Where position is represented by $x(t)$, t is time and t_f is the final time. C_k s are parameters that depend on the boundary motion states and on the time between them, t_f . They can be found by solving the boundary conditions on the motion state.

Once the coefficients are determined the cumulative squared jerk can be computed by simply integrating the squared jerk profile.

$$j(t) = \dot{x}(t) = [60C_5(t/t_f)^2 + 24C_4(t/t_f) + 6C_3]/t_f^3$$

$$\text{Cumulative Squared Jerk} = \int_0^{t_f} j^2(t) dt$$

Received 26 August; accepted 3 November 1999.

1. Folstein, S. E. *Huntington's Disease a Disorder of Families* (Johns Hopkins Univ. Press, Baltimore, 1989).
2. The Huntington's Disease Collaborative Research Group. A novel gene containing a trinucleotide repeat that is expanded and unstable on Huntington's disease chromosomes. *Cell* **72**, 971–983 (1993).
3. Aylward, E. H. et al. Longitudinal change in basal ganglia volume in patients with Huntington's disease. *Neurology* **48**, 394–399 (1997).
4. Aylward, E. H. et al. Basal ganglia volume and proximity to onset in presymptomatic Huntington disease. *Arch Neurol* **53**, 1293–1296 (1996).
5. Brandt, J. et al. Clinical correlates of dementia and disability in Huntington's disease. *J. Clin. Neuropsychol.* **6**, 401–412 (1984).
6. Shadmehr, R. & Mussa-Ivaldi, F. A. Adaptive representation of dynamics during learning of a motor task. *J. Neurosci.* **14**, 3208–3224 (1994).
7. Shidara, M., Kawano, K., Gomi, H. & Kawato, M. Inverse-dynamics model eye movement control by Purkinje cells in the cerebellum. *Nature* **365**, 50–52 (1993).
8. Bhushan, N. & Shadmehr, R. Computational nature of human adaptive control during learning of reaching movements in force fields. *Biol. Cybern.* **81**, 39–60 (1999).
9. Shadmehr, R. & Brashers-Krug, T. Functional stages in the formation of human long-term motor memory. *J. Neurosci.* **17**, 409–419 (1997).
10. Flash, T. & Hogan, N. The coordination of arm movements: an experimentally confirmed mathematical model. *J. Neurosci.* **5**, 1688–1703 (1985).
11. Miall, R. C., Weir, D. J. & Stein, J. F. Manual tracking of visual targets by trained monkeys. *Behav. Brain Res.* **20**, 185–201 (1986).
12. Wolpert, D. M., Ghahramani, Z. & Jordan, M. I. Are arm trajectories planned in kinematic or dynamic coordinates? An adaptation study. *Exp. Brain Res.* **103**, 460–470 (1995).
13. Cordo, P. J. Kinesthetic control of a multijoint movement sequence. *J. Neurophysiol.* **63**, 161–172 (1990).
14. Atkeson, C. G. & Hollerbach, J. M. Kinematic features of unrestrained vertical arm movements. *J. Neurosci.* **59**, 2318–2330 (1985).
15. Meyer, B. U. et al. Motor responses evoked by magnetic brain stimulation in Huntington's Disease. *Electroencephalogr. Clin. Neurophysiol.* **85**, 197–208 (1992).
16. Noth, J., Podoll, K. & Friedemann, H. H. Long-loop reflexes in small hand muscles studied in normal subjects and in patients with Huntington's Disease. *Brain* **108**, 65–80 (1985).
17. Kuwert, T. et al. Comparison of somatosensory evoked potentials with striatal glucose consumption measured by positron emission tomography in the early diagnosis of Huntington's Disease. *Mov. Disord.* **8**, 98–106 (1993).
18. Topper, R., Schwarz, M., Podoll, K., Domges, F. & Noth, J. Absence of frontal somatosensory evoked potentials in Huntington's Disease. *Brain* **116**, 87–101 (1993).
19. Foroud, T. et al. Cognitive scores in carriers of Huntington's disease gene compared to noncarriers. *Ann. Neurol.* **37**, 657–664 (1995).
20. de Boo, G. M. et al. Early cognitive and motor symptoms in identified carriers of the gene for Huntington disease. *Arch. Neurol.* **54**, 1353–1357 (1997).
21. Siemers, E. et al. Motor changes in presymptomatic Huntington disease gene carriers. *Arch. Neurol.* **53**, 487–492 (1996).
22. Rothlind, J. C., Brandt, J., Zee, D., Codori, A. M. & Folstein, S. Unimpaired verbal memory and oculomotor control in asymptomatic adults with the genetic marker for Huntington's disease. *Arch. Neurol.* **50**, 799–802 (1993).
23. Blackmore, L., Simpson, S. A. & Crawford, J. R. Cognitive performance in UK sample of presymptomatic people carrying the gene for Huntington's disease. *J. Med. Genet.* **32**, 358–362 (1995).
24. Kuwert, T. et al. Striatal glucose consumption in chorea-free subjects at risk of Huntington's disease. *J. Neurol.* **241**, 31–36 (1993).
25. Mazziootta, J. C. et al. Reduced cerebral glucose metabolism in asymptomatic subjects at risk for Huntington's Disease. *N. Engl. J. Med.* **316**, 357–362 (1987).

26. Gabrieli, J. D., Stebbins, G. T., Singh, J., Willingham, D. B. & Goetz, C. G. Intact mirror-tracing and impaired rotary-pursuit skill learning in patients with Huntington's Disease: Evidence for dissociable memory systems in skill learning. *Neuropsychology* **11**, 272–281 (1997).
27. Hogan, N. in *Multiple Muscle Systems* (eds Winters, J. M. & Woo, S. L. Y.) 149–164 (Springer, New York, 1990).
28. Miall, R. C. & Wolpert, D. M. Forward models for physiologic motor control. *Neur. Net.* **9**, 1265–1279 (1996).
29. Schultz, W., Dayan, P. & Montague, P. R. A neural substrate of prediction and reward. *Science* **275**, 1593–1599 (1997).

Acknowledgements

We thank K. Thoroughman and N. Bhushan. R.S. and M.S. conceived of the experiments, M.S. collected the data, and designed and carried out the data analysis guided by interaction with R.S., J.B., N.B. and K.T. M.S. and R.S. wrote the manuscript. The Johns Hopkins HD Center (director C. A. Ross) arranged patient visits and clinical assessment of HD patients. The work was supported by grants from the Whitaker Foundation (R.S.) and the National Institutes of Health (R.S. and J.B.), and a pre-doctoral fellowship from the National Institute of General Medical Sciences to M.S.

Correspondence and requests for materials should be addressed to M.S. (e-mail: msmith@bme.jhu.edu).

.....
A neuronal analogue of state-dependent learning

D. E. Shulz^{*}, R. Sosnik[†], V. Ego^{*}, S. Haidarliu[†] & E. Ahissar[†]

[†] Department of Neurobiology, The Weizmann Institute of Science, 76100 Rehovot, Israel

^{*} Equipe Cognisciences, UNIC, Institut A. Fessard, CNRS, 91198 Gif sur Yvette, France

.....
State-dependent learning is a phenomenon in which the retrieval of newly acquired information is possible only if the subject is in the same sensory context and physiological state as during the encoding phase¹. In spite of extensive behavioural and pharmacological characterization², no cellular counterpart of this phenomenon has been reported. Here we describe a neuronal analogue of state-dependent learning in which cortical neurons show an acetylcholine-dependent expression of an acetylcholine-induced functional plasticity. This was demonstrated on neurons of rat somatosensory 'barrel' cortex, whose tunings to the temporal frequency of whisker deflections were modified by cellular conditioning. Pairing whisker stimulation with acetylcholine applied iontophoretically yielded selective lasting modification of responses, the expression of which depended on the presence of exogenous acetylcholine. Administration of acetylcholine during testing revealed frequency-specific changes in response that were not expressed when tested without acetylcholine or when the muscarinic antagonist, atropine, was applied concomitantly. Our results suggest that both acquisition and recall can be controlled by the cortical release of acetylcholine.

The ascending cholinergic system³ has long been considered to be a candidate for mediating behavioural control of neuronal plasticity^{4–9}. This hypothesis is supported by behavioural and neurophysiological studies in the auditory^{10–13} and somatosensory systems^{14–18}. Whereas these studies demonstrated the permissive role of acetylcholine (ACh) during the induction of cortical plasticity^{10–14}, they did not address the possibility that ACh is also involved in the expression of the induced modifications. To examine this potential role of ACh, single- ($n = 99$) and multi-unit ($n = 85$) activities were recorded extracellularly from the barrel field¹⁹ of anaesthetized adult rats, using a multi-electrode array composed of one or two tungsten-in-glass electrodes and one combined electrode for recording and iontophoresis of ACh. Temporal-frequency tuning curves (TFTCs)